Vascular Caveolin Deficiency Supports the Angiogenic Effects of Nitrite, a Major End Product of Nitric Oxide Metabolism in Tumors

Françoise Frérart,[1] Irina Lobysheva,[1] Bernard Gallez,[2] Chantal Dessy,[1] and Olivier Feron[1]

[1]Unit of Pharmacology and Therapeutics, Université Catholique de Louvain, UCL-FATH 5349; [2]Unit of Biomedical Magnetic Resonance, Université Catholique de Louvain, UCL-REMA 7340, Brussels, Belgium

Abstract

The biological status of nitrite recently evolved from an inactive end product of nitric oxide (NO) metabolism to a major intravascular and tissue storage of NO. Several enzymes and proteins may indeed work as nitrite reductases. The endothelial NO synthase (eNOS) is proposed to be one of them, particularly when oxygen is lacking. Here, we examined whether the lack of caveolin, a scaffold protein known to limit eNOS activity under basal conditions and to be down-regulated in tumor vessels, could favor the reconversion of nitrite into NO and thereby promote angiogenesis. We found that nitrite-rich serum from caveolin-deficient mice and exogenous nitrite exert proangiogenic effects on aortic explants cultured in a three-dimensional collagen matrix. We identified a higher intrinsic capacity of caveolin-deficient vessels and endothelial cells to convert nitrite into bioactive NO. These effects did occur under moderate hypoxia and were abolished on exposure to a NO scavenger. Evidence for eNOS acting as a nitrite reductase derived from the failure to reproduce the proangiogenic effects of nitrite on eNOS-deficient aorta rings and endothelial cells. Finally, in a mouse tumor model, we documented the higher nitrite content in hypoxic tumors and identified inducible NO synthase as the major source of nitrite. Altogether, these data identify the lack of caveolin observed in the tumor vasculature as a favorable ground for nitrite-driven formation of endothelial tubes in the hypoxic tumor microenvironment. This work also strengthens the therapeutic value of the modulation of caveolin expression to interfere with tumor angiogenesis. (Mol Cancer Res 2009;7(7):1056–63)

Introduction

Nitric oxide (NO) plays a major role in many key pathophysiologic processes, including the control of vascular tone (1) and angiogenesis (2). Although nitrites and nitrates have been described for a long time as the inert end products of the NO oxidative metabolism (3), recent evidence indicates that under specific conditions nitrite can be reconverted into biologically active NO (4). The nitrite anion is now considered as the largest intravascular and tissue storage of NO, which may be made available depending on the tissue need. Nitrite was for instance shown to contribute to hypoxic vasodilation (5-7) and to protect several organs, including heart, liver, kidney, and brain, from ischemia-reperfusion injuries (8-13). Different pathways are proposed to support the reductive reconversion of nitrite into NO. Besides the acidic reduction/disproportionation of nitrite species (14-16), some heme-containing enzymes, including deoxyhemoglobin (7, 17, 18) and xanthine oxidase (19, 20), can act as nitrite reductases under hypoxia, thereby offering a salvage pathway to produce NO when oxygen-consuming NO synthases (NOS) become inoperative.

Interestingly, the endothelial NOS (eNOS) isoform itself, in the absence of oxygen, has been shown to behave as a nitrite reductase (21, 22). In endothelial cells, the catalytic eNOS activity is regulated by caveolin-1, the structural protein of flask-shaped plasma membrane invaginations named caveolae. The physical interaction of eNOS with the so-called caveolin-1 scaffolding domain maintains the enzyme in an inactivated state (23-26), preventing the activation of eNOS in basal (unstimulated) conditions. In tumors, we recently reported that a deficit in the expression of caveolin in tumor blood vessels was associated with an exacerbated angiogenesis (27). Although caveolin-free eNOS as a direct source of NO (endowed with potent angiogenic properties) may account for the observed increase in tumor neovascularization, the low pO_2 in tumors should, however, alter the capacity of the enzyme to produce NO. Here, we examined the alternative hypothesis according to which nitrite reconverted into NO by caveolin-free eNOS in tumor blood vessels could support angiogenesis occurring under hypoxia. We used the so-called *ex vivo* aorta ring assay where pieces of freshly dissected mouse aorta are embedded in collagen and cultured in a medium complemented with serum.

We found that the lack of caveolin-1 expression leads to an extended sensitivity of vessels to nitrite exposure and consecutively favors NO-dependent angiogenesis under hypoxic conditions. As a decrease in caveolin-1 expression was reported in endothelial cells lining tumor blood vessels (27, 28), these findings underline the potential of nitrite in promoting angiogenesis
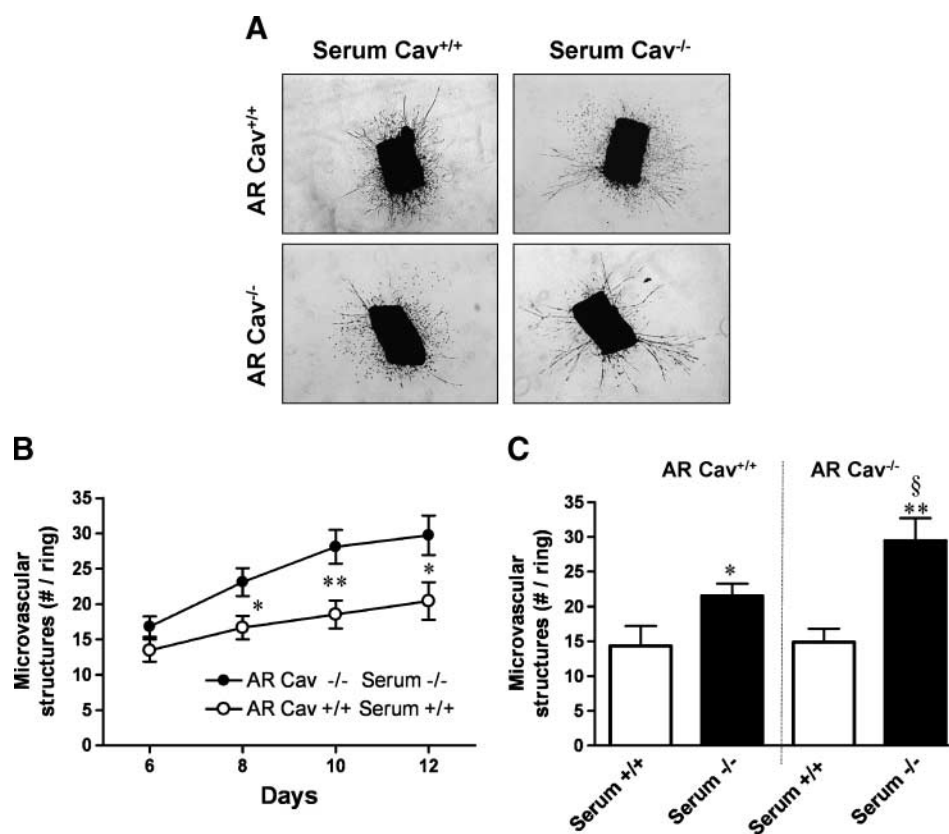
FIGURE 1. Serum from Cav$^{-/-}$ mice is highly proangiogenic. Collagen-embedded aortic rings from Cav$^{+/+}$ and Cav$^{-/-}$ mice were cultured in the presence of Cav$^{+/+}$ or Cav$^{-/-}$ serum. **A.** Representative pictures of Cav$^{+/+}$ (*top*) and Cav$^{-/-}$ (*bottom*) aortic rings (*AR*) cultured in the presence of Cav$^{+/+}$ (*left*) or Cav$^{-/-}$ (*right*) serum; pictures were obtained after 10 d of culture. **B.** Number (after 6, 8, 10, and 12 d of culture) of linear microvascular structures outgrowing from Cav$^{+/+}$ (○) and Cav$^{-/-}$ (●) aortic rings cultured in the presence of Cav$^{+/+}$ and Cav$^{-/-}$ serum, respectively. Points, mean; bars, SE. *, $P < 0.05$; **, $P < 0.01$ ($n = 28$ for each condition from at least 15 different aortas per genotype). **C.** Number of microvasculature structures (after 12 d of culture) outgrowing from Cav$^{+/+}$ (*left*) and Cav$^{-/-}$ (*right*) aortic rings cultured in the presence of Cav$^{+/+}$ (*white columns*) or Cav$^{-/-}$ (*black columns*) serum. Columns, mean; bars, SE. *, $P < 0.05$; **, $P < 0.01$ versus corresponding Cav$^{+/+}$ serum conditions; §, $P < 0.05$ versus Cav$^{+/+}$ aorta ring and Cav$^{-/-}$ serum condition ($n = 6-12$ from six different aortas per genotype).

in the hypoxic tumor microenvironment and strengthen the need for strategies targeting NO production in tumors to affect cancer progression.

Results

Serum from Cav$^{-/-}$ Mice Is Highly Proangiogenic

To assess whether caveolin down-regulation, as observed in tumor blood vessels, could regulate angiogenesis, sera from Cav$^{+/+}$ and Cav$^{-/-}$ mice were used to stimulate vascular outgrowth from aortic rings (themselves collected from Cav$^{+/+}$ and Cav$^{-/-}$ mice). Aorta rings were embedded in collagen gels and cultured in the presence of autologous serum (i.e., Cav$^{+/+}$ serum for Cav$^{+/+}$ explants and Cav$^{-/-}$ serum for Cav$^{-/-}$ explants). As shown in Fig. 1A and B, the outgrowth of microvascular structures was more extensive from Cav$^{-/-}$ aorta than from Cav$^{+/+}$ explants. To discriminate between the respective influence of the explants and the serum on the promotion of angiogenesis, Cav$^{+/+}$ and Cav$^{-/-}$ aortic rings were also cultured in the presence of heterologous serum (i.e., Cav$^{-/-}$ serum for Cav$^{+/+}$ explants and Cav$^{+/+}$ serum for Cav$^{-/-}$ explants). As presented in Fig. 1A and C, Cav$^{-/-}$ serum promoted outgrowth of

microvascular structures from both genotype explants to a higher extent than wild-type serum. Cav$^{-/-}$ serum did, however, induce the outgrowth of more endothelial structures from Cav$^{-/-}$ than from Cav$^{+/+}$ explants.

Cav$^{-/-}$ Mouse Serum Contains Higher Amounts of Nitrite (than Wild-Type Serum)

To determine the nature of the proangiogenic factors present in the Cav$^{-/-}$ mouse serum, we used protein array membranes designed to evaluate the abundance of major proangiogenic and antiangiogenic actors. In this assay, no critical differences were found in the composition of sera from Cav$^{+/+}$ and Cav$^{-/-}$ mice (Fig. 2A). We then focused on the major difference between Cav$^{+/+}$ and Cav$^{-/-}$ mouse vessels: the unclamping of eNOS from its inhibitory interaction with caveolin in endothelial cells and the consecutive increase in eNOS activity (23, 29). We found that, indeed, agonist-induced NO release from Cav$^{-/-}$ aorta amounted to ∼160% of the NO production in wild-type vessels (Fig. 2B) and that a ∼3-fold increase in serum nitrite concentration was found in Cav$^{-/-}$ mice (versus Cav$^{+/+}$ mice; Fig. 2C). The L-NAME sensitivity of the NO measurement confirmed that changes in eNOS activity did account for the

observed differences (Fig. 2B); note that no change in eNOS protein abundance was observed according to the two mouse genotypes (data not shown).

Exogenous Nitrite Stimulates Angiogenesis from Ex vivo Hypoxic Vessels

As nitrite can reform biologically active NO (which in turn may exert proangiogenic effects), we then examined whether the treatment of aorta rings with nitrite could recapitulate the effects of $Cav^{-/-}$ serum. As shown in Fig. 3A and B, addition of exogenous nitrite led to a dramatic increase in endothelial outgrowth from $Cav^{-/-}$ aorta rings.

Based on the above results, we suspected that eNOS was acting as a nitrite reductase in our model. We therefore aimed to examine whether hypoxia (a prerequisite for such activity) was present in our experimental conditions. We evaluated the expression of carbonic anhydrase IX (CAIX) as a reporter of hypoxia in our models of embedded aorta rings (wherein oxygen gradient could develop through the collagen gel). Although

experiments were done under normoxic conditions (5% CO_2/95% air in the incubator), the CAIX immunostaining was found to be higher when explants were embedded in collagen compared with explants freshly isolated or cultured but non-embedded (Fig. 4A and B). Aortic rings submitted to 1% hypoxia were used as positive controls for the induction of CAIX expression. Of note, electron paramagnetic resonance measurements using lithium phthalocyanine as an oxygen-sensitive paramagnetic probe also indicated that the pO_2 in collagen-embedded aorta was consistently found to be ∼15 mm Hg (despite technical limitations linked to the processing of the vessel out of the incubator).

Nitrite-Fueled eNOS Drives Angiogenesis under Hypoxia

To document the role of eNOS as a major nitrite reductase in our *ex vivo* assay, we used aorta rings from eNOS-deficient mice. As shown in Fig. 4C, we observed that nitrite failed to stimulate vascular outgrowth from $eNOS^{-/-}$ aorta rings. We then measured the capacity of $eNOS^{-/-}$, $Cav^{-/-}$, and wild-type mouse aorta
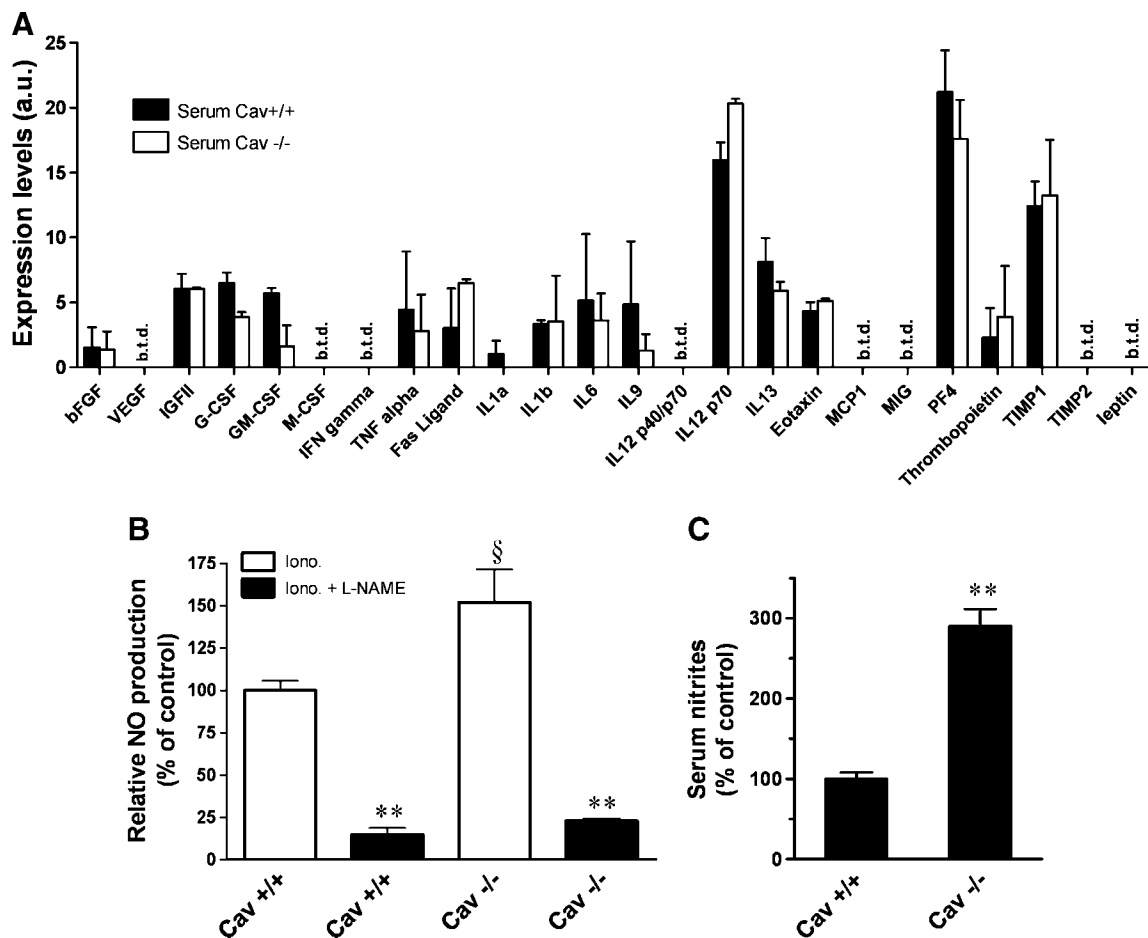

FIGURE 2. $Cav^{-/-}$ and $Cav^{+/+}$ mouse sera differ in their nitrite content. **A.** Mean expression level [arbitrary unit (*a.u.*)] of each protein detected from $Cav^{+/+}$ (*black columns*) and $Cav^{-/-}$ (*white columns*) sera after incubation on the array membranes (two spots per membrane for each protein). b.t.d., below threshold of detection. **B.** NO production from $Cav^{+/+}$ and $Cav^{-/-}$ aorta in response to ionomycin with or without L-NAME. Aortas were treated or not with L-NAME and incubated with colloid [Fe(II)(DETC)$_2$] and ionomycin (2 µmol/L) for 30 min at 37°C. Data are quantified from the EPR signals of [Fe(II)NO(DETC)$_2$] in aortic rings and normalized to the weight of dry aortas (n = 3-4). **, $P < 0.01$ versus corresponding ionomycin conditions; §, $P < 0.05$ versus ionomycin-treated $Cav^{+/+}$ aorta. **C.** Plasma nitrite concentration in $Cav^{+/+}$ and $Cav^{-/-}$ mice. Data are expressed as percentage of the control ($Cav^{+/+}$) condition. Columns, mean; bars, SE. **, $P < 0.01$ (n = 3).
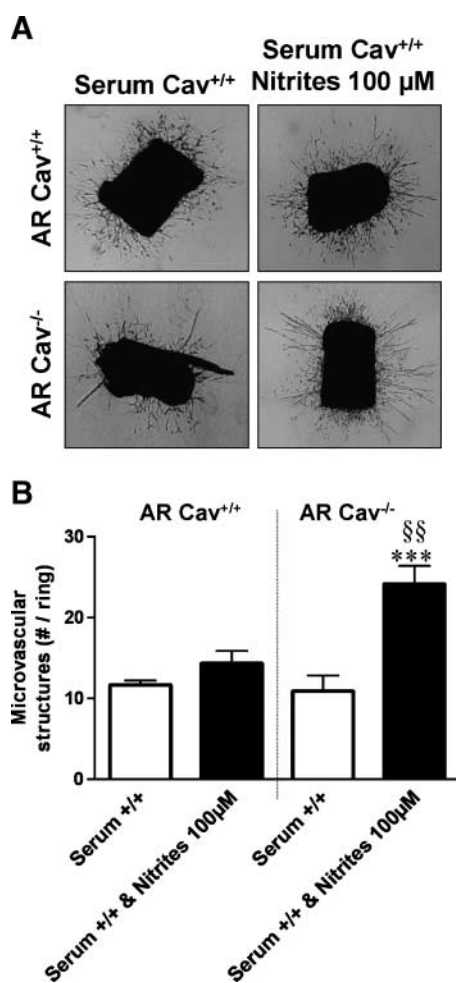
FIGURE 3. Nitrite exerts proangiogenic effects in a caveolin-dependent manner. Collagen-embedded aortic rings from Cav$^{+/+}$ and Cav$^{-/-}$ mice were cultured in the presence of Cav$^{+/+}$ serum alone or with 100 μmol/L nitrite. **A.** Representative pictures of Cav$^{+/+}$ (*top*) and Cav$^{-/-}$ (*bottom*) aortic rings cultured with Cav$^{+/+}$ serum alone (*left*) or in the presence of 100 μmol/L nitrite (*right*); pictures were obtained after 8 d of culture. **B.** Number of linear microvascular structures (after 8 d of culture) outgrowing from Cav$^{+/+}$ (*left*) and Cav$^{-/-}$ (*right*) aortic rings cultured in the presence of Cav$^{+/+}$ serum with (*black columns*) or without (*white columns*) 100 μmol/L nitrite. Columns, mean; bars, SE. ***, $P < 0.001$ versus corresponding Cav$^{+/+}$ serum condition; §§, $P < 0.01$ versus Cav$^{+/+}$ serum and nitrite condition (n = 6-9 from four different aortas per genotype).

rings to convert L-arginine into NO. Such measurements of the catalytic eNOS activity led to the observation that collagen embedding largely prevented the NOS activity (see *white columns* in Fig. 4D). Interestingly, exposure of wild-type and Cav$^{-/-}$ aorta rings to high O$_2$ concentrations led to a net stimulation of NOS activity in this assay (see *black columns* in Fig. 4D); the eNOS$^{-/-}$ aorta rings completely failed to reveal NOS activity. Note also that the extent of L-arginine conversion was not significantly different between Cav$^{-/-}$ and wild-type mouse aorta and that this oxidative NO-producing pathway could thus not account for the difference in the extent of angiogenesis observed between these two conditions (see Fig. 4C). We also exploited the capacity of endothelial cells to form tubes when cultured on Matrigel to evaluate whether the combination of hypoxia and exogenous nitrite could modulate angiogenesis. In this other assay, hypoxic

conditions (1% O$_2$) failed to stimulate basal angiogenesis from wild-type endothelial cells (see *hatched columns* in Fig. 4E). We found, however, that the addition of 100 μmol/L nitrite significantly stimulated endothelial tubulogenesis, reaching 20% of the effects observed under normoxia. Caveolin-1 silencing using a dedicated small interfering RNA (siRNA) further increased by 2-fold the extent of tube formation from endothelial cells exposed to hypoxia in the presence of nitrite (Fig. 4E). Caveolin deficiency barely influences, in this model, the extent of basal angiogenesis under normoxia. Finally, using endothelial cells isolated from eNOS$^{-/-}$ mice, we confirmed the key role of this enzyme in both normoxic and hypoxic conditions to drive angiogenesis because we did not observe any significant tube formation by plating theses cells on Matrigel (Fig. 4E). Moreover, caveolin silencing in these eNOS$^{-/-}$ endothelial cells did not have any effect on the capacity of nitrite to stimulate angiogenesis under hypoxia (Fig. 4E).

Ex vivo *Angiogenesis from Aortic Explants Is NO Dependent*

To assess the NO dependence of both the Cav$^{-/-}$ serum and the exogenous nitrite-induced angiogenesis in our *ex vivo* model, we exposed aorta ring cultures to 100 μmol/L NO scavenger (C-PTIO). We found that C-PTIO abrogated the stimulation of the vascular outgrowth observed in response to Cav$^{+/+}$ serum complemented with exogenous nitrite (100 μmol/L; see Fig. 5A and B). Importantly, C-PTIO also reduced by 60% the microvascular structure outgrowth from aorta rings exposed to Cav$^{-/-}$ serum, confirming the NO dependency of the pathway induced by nitrite-rich serum (Fig. 5A and B); vehicle (DMSO) had no effect on the extent of endothelial outgrowth (data not shown).

Nitrite Accumulates in Hypoxic Tumors in Response to Inducible NO Synthase Expression

We have compared the nitrite content in tumors grown in Cav$^{-/-}$ and Cav$^{+/+}$ mice. We found a slight but reproducible 20% increase in Cav$^{-/-}$ tumors (Fig. 6A). We also documented that the nitrite concentration was 5-fold higher in tumors than in the surrounding muscle (Fig. 6B). Using the specific inducible NO synthase (iNOS) inhibitor 1400W, we found that most of the tumor versus muscle difference arose from iNOS activity (Fig. 6B). Finally, using pools of tumors of small and large diameters, we collected tumors with different O$_2$ status, as determined by electronic paramagnetic resonance (EPR), and found that hypoxic tumors were associated with larger nitrite contents (Fig. 6C).

Discussion

In this study, we found that the reduction in caveolin abundance known to occur in tumor vessels (27, 28, 30) is prone to favor NO-mediated angiogenesis from nitrite. The *ex vivo* model of serum-driven vascular outgrowth from aorta rings was critical to identify how nitrite could take advantage of a caveolin-unclamped eNOS to promote angiogenesis. The higher angiogenic potential of the serum collected from Cav$^{-/-}$ mice (versus wild-type mice) was the seminal finding that led us to identify nitrite as key actor supporting vascular outgrowth. As a preamble to this discussion, it should, however, be stressed that the increase in serum nitrite concentration in Cav$^{-/-}$ mice arises from the overall increase in eNOS activity

in all the vascular beds of the animal and therefore does not reflect a naturally occurring systemic increase in nitrite in response to local tumor growth. The accumulation of nitrite, as a major end product of the NO catabolism, in tumors may actu-

ally arise from the activation of any NOS isoform. We and others have previously reported that the abundance of caveolin, the scaffold protein regulating eNOS activity (23, 29), was reduced in the tumor vasculature (27, 28, 30), thereby promoting
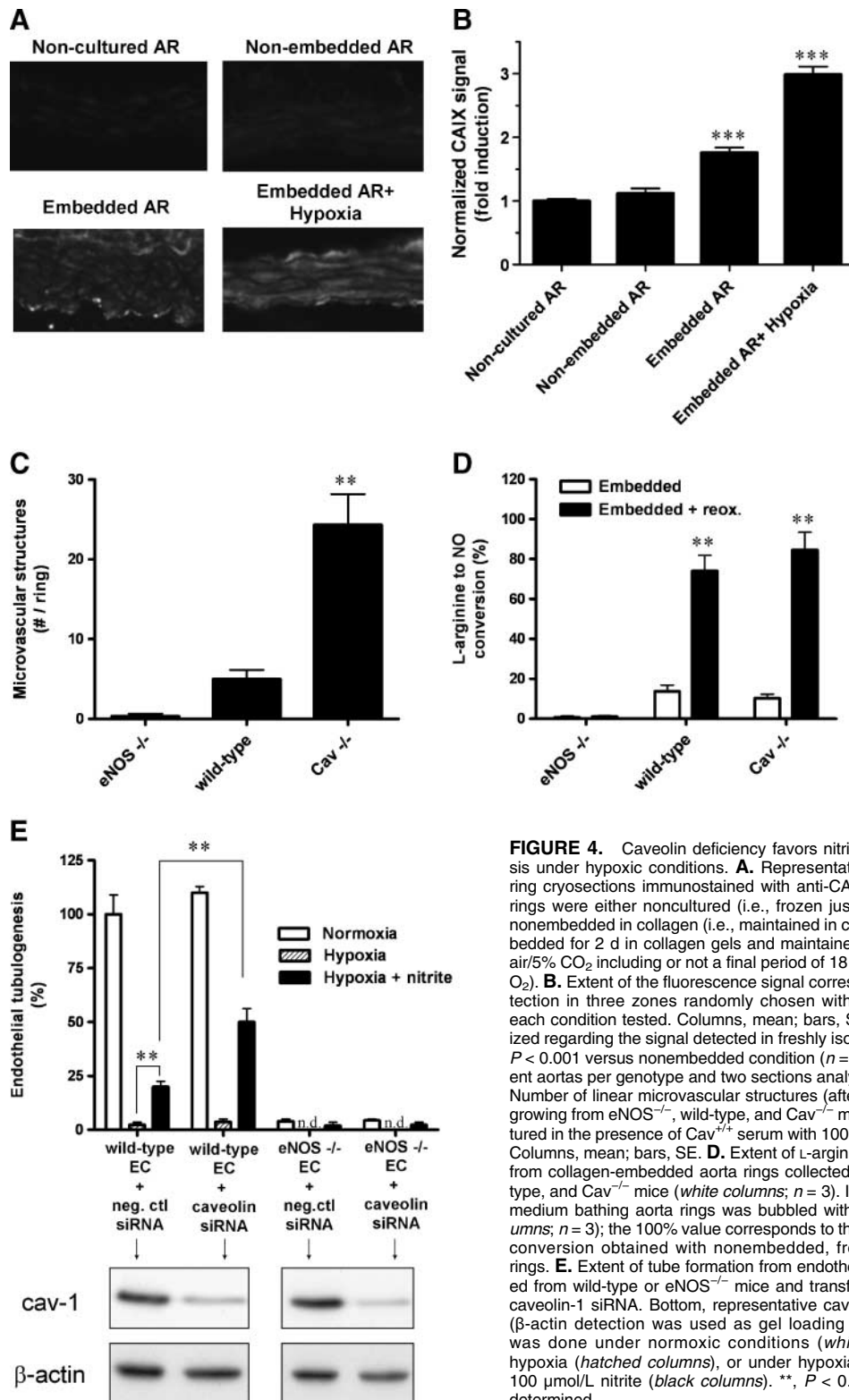

FIGURE 4. Caveolin deficiency favors nitrite-driven angiogenesis under hypoxic conditions. **A.** Representative pictures of aorta ring cryosections immunostained with anti-CAIX antibodies. Aortic rings were either noncultured (i.e., frozen just after collection), or nonembedded in collagen (i.e., maintained in culture for 2 d), or embedded for 2 d in collagen gels and maintained for 2 d under 95% air/5% CO_2 including or not a final period of 18 h under hypoxia (1% O_2). **B.** Extent of the fluorescence signal corresponding to CAIX detection in three zones randomly chosen within the aorta wall for each condition tested. Columns, mean; bars, SE. Data are normalized regarding the signal detected in freshly isolated aorta rings. ***, $P < 0.001$ versus nonembedded condition ($n = 3-5$ from three different aortas per genotype and two sections analyzed per explant). **C.** Number of linear microvascular structures (after 8 d of culture) outgrowing from eNOS$^{-/-}$, wild-type, and Cav$^{-/-}$ mouse aortic rings cultured in the presence of Cav$^{+/+}$ serum with 100 μmol/L nitrite ($n = 3$). Columns, mean; bars, SE. **D.** Extent of L-arginine conversion to NO from collagen-embedded aorta rings collected from eNOS$^{-/-}$, wild-type, and Cav$^{-/-}$ mice (white columns; $n = 3$). In some experiments, medium bathing aorta rings was bubbled with 95% O_2 (black columns; $n = 3$); the 100% value corresponds to the extent of L-arginine conversion obtained with nonembedded, freshly isolated aorta rings. **E.** Extent of tube formation from endothelial cells (EC) isolated from wild-type or eNOS$^{-/-}$ mice and transfected (or not) with a caveolin-1 siRNA. Bottom, representative caveolin immunoblotting (β-actin detection was used as gel loading control). The assay was done under normoxic conditions (white columns), under hypoxia (hatched columns), or under hypoxia in the presence of 100 μmol/L nitrite (black columns). **, $P < 0.01$ ($n = 3$). n.d., not determined.
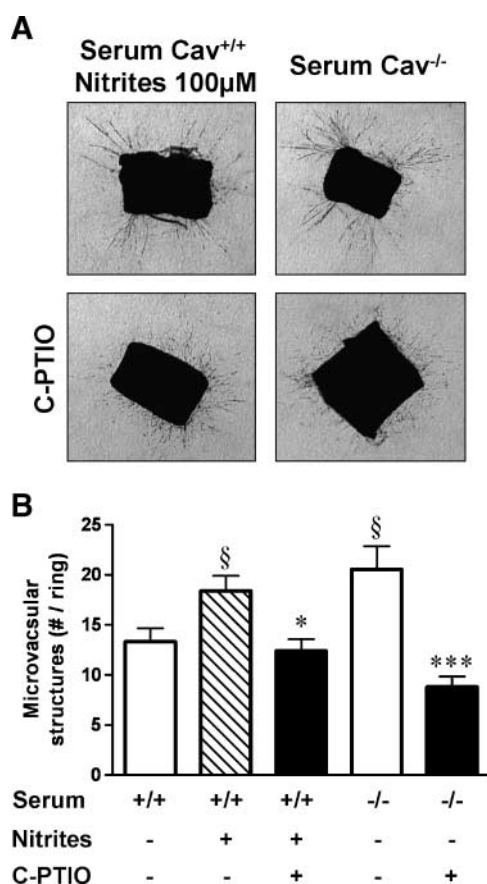
A

B

FIGURE 5. NO scavenging prevents the angiogenic effects of nitrite. Collagen-embedded aortic rings from Cav$^{-/-}$ mice were cultured either in the presence of Cav$^{+/+}$ serum (complemented or not with 100 μmol/L nitrite) or in the presence of Cav$^{-/-}$ serum. **A.** Representative pictures of aortic rings cultured in the presence of Cav$^{+/+}$ serum + nitrite (*left*) and in the presence of Cav$^{-/-}$ serum (*right*). Bottom, effects of 100 μmol/L C-PTIO. Pictures were obtained after 6 d of culture. **B.** Number of linear microvascular structures outgrowing (after 6 d of cultures) from aortic rings cultured in the indicated conditions. Columns, mean; bars, SE. §, $P < 0.05$ versus Cav$^{+/+}$ serum alone; *, $P < 0.05$; ***, $P < 0.001$ versus respective condition without C-PTIO ($n = 5$-12).

the endothelial NO production in tumors. High levels of NO production may also result from iNOS-expressing tumor-associated macrophages (31, 32) or directly from neuronal NOS–expressing tumor cells (33); some tumor cells were also reported to express iNOS or eNOS (34). In the current study, using a mouse tumor model wherein tumor cells do not express any NOS isoform, we documented that the major contribution of host cells in the production of nitrites by the tumor arose from iNOS (Fig. 6).

The fate of nitrite is normally to be eliminated in the urine after transiting into the bloodstream. In ischemic cardiovascular tissues, it was, however, recently documented that infused nitrite could contribute to reform a bioactive NO pool and participate to the recovery of ischemic tissues (35, 36). Our data indicate that nitrite-derived NO may exert its effects by stimulating angiogenesis. This may participate in the reduction of postischemic damages in cardiovascular tissues but also in the development of tumor neovascularization. Among the enzyme candidates for the reconversion of nitrite into NO, our

work on Cav$^{-/-}$ mice indicates that eNOS may act as a nitrite reductase, particularly when the abundance of the endogenous inhibitor caveolin is reduced and under hypoxic conditions. The combination of these two factors is critical. Indeed, *in vitro* data previously documented that under complete anoxia, eNOS could contribute to reconvert nitrite into NO (21, 22). In our experimental model of aorta rings, hypoxia is present, as verified by CAIX staining and EPR oximetry probe, but should be viewed as a moderate form of hypoxia because it is the embedding of aorta rings into the collagen (and not the strict lack of O_2) that limits the O_2 diffusion to the vessel from the ambient incubator 95% air-5% CO_2 gas mixture. Importantly, we showed that this form of diffusion-limited hypoxia was sufficient to prevent significant conversion of L-arginine into NO (i.e., normal eNOS catalytic activity) and could be reversed by increasing oxygen concentration in the medium bathing embedded aorta rings (Fig. 4C).

We and others previously documented that tumor angiogenesis was exacerbated in tumor growing in Cav$^{-/-}$ mice (27, 37). The current data support the contribution of NO—through nitrite reconversion—to the neovascularization process occurring in tumor hypoxic regions. Using cultured endothelial cells exposed to caveolin-targeting siRNA, we showed that although the extent of angiogenesis was lower than in normoxic conditions, the caveolin down-regulation promoted the angiogenic effects of the combination of exogenous nitrite and hypoxia (Fig. 4E).

In conclusion, our data identify the angiogenic potential of nitrite in tumors and unravel how eNOS-mediated signaling may occur in hostile, hypoxic conditions, as encountered in many tumors. This study also strengthens the therapeutic value of caveolin reexpression (38) or caveolin-derived peptide administration (39, 40) to selectively block eNOS activity in tumors.

Materials and Methods

Mice

Caveolin-1–deficient (Cav$^{-/-}$) mice (originally obtained from Dr. T.V. Kurzchalia, Max Planck Institute for Molecular Cell Biology and Genetics, Dresden, Germany; ref. 41) and their control littermates (Cav$^{+/+}$) were generated through heterozygous matings and housed in our local facility. eNOS-deficient (eNOS$^{-/-}$) mice were obtained from Charles River Laboratories. NMRI, male mice (Elevage Janvier) were used in experiments with syngeneic TLT carcinoma cells (42, 43). Mice received an i.m. injection of 10^5 tumor cells in the posterior right leg. The tumor diameters were tracked with an electronic caliper. In some experiments, mice received the iNOS-selective inhibitor 1400W (50 mg/L in the drinking water). Each procedure was approved by the local authorities according to national animal care regulations.

Three-Dimensional Aortic Ring Assay

Preparation of three-dimensional aortic ring cultures was made as previously described (44). Briefly, blood and aorta were collected from anesthetized mice. Cleaned aortic rings (1-mm long) were then embedded in a collagen type I matrix and cultured in the presence of MCDB131 medium supplemented with 25 mmol/L NaHCO$_3$, 2.5% mouse serum, 1% glutamine, 100 units/mL penicillin, and 100 μg/mL streptomycin. In

each experiment, mouse sera were pooled in accordance with genotype. Digital images of microvascular structure outgrowth were obtained with the use of a Zeiss inverted microscope coupled to a charge-coupled device camera on days 6, 8, 10, and 12. Angiogenesis quantification was done by counting the number of microvascular structures grown out of each aortic explant. Nitrite ($NaNO_2$; Fluka) and C-PTIO [2-(4-carboxyphenyl)-4,4,5,5-tetramethylimidazoline-1-oxyl-3-oxide potassium salt; Sigma] were added at the day of the culture preparation.

Tubulogenesis Assay

Endothelial cells were obtained from wild-type and $eNOS^{-/-}$ mouse aorta according to the primary explant procedure, as previously reported (45). Endothelial cell reorganization in capillary-like structures was observed, after plating on Matrigel, using an inverted phase-contrast microscope and the length of the endothelial network was quantified by analysis of images randomly captured by a video camera system. In some experiments, endothelial cells were transfected with duplex siRNA targeting caveolin-1 (corresponding to the coding sequence 206-226) using Lipofectin (Invitrogen), according to the manufacturer's protocol. A negative control siRNA was used as control and a minimum 90% reduction in caveolin-1 expression level was validated by immunoblotting done in parallel to the assay, as described elsewhere (27). For hypoxic conditions, cells were incubated in a gas-regulated (1% O_2, 94% N_2, 5% CO_2) workstation (InVivo 500, Ruskinn).

Protein Array

Mouse Angiogenesis Antibody Array I (RayBiotech, Inc.) was used to compare the relative amounts of different angiogenesis regulator proteins present in the sera of $Cav^{-/-}$ and $Cav^{+/+}$ mice. Sera were collected from mice just as for the three-dimensional aortic ring cultures. Blood sera from three animals per genotype were pooled and screened for cytokine expression, according to the manufacturer's protocol. Quantification was done by densitometry using ImageJ 1.37v (NIH).

Immunostaining

After 2 d of culture, aortic rings were drawn from the collagen gels with fine forceps and quickly frozen in liquid nitrogen for cryoslicing. Rings were also either directly snap frozen or cultured (nonembedded) in complete MCDB131 medium for 2 d. In some experiments, embedded aortic rings were submitted to hypoxia (1% O_2) for 18 h in a modular incubator chamber (Billups Rothenberg, Inc.) used as previously described (43). Green autofluorescence of elastic fibers in the aorta wall was quenched using Chicago Sky Blue 6B 0.5% (Sigma), and sections were then probed with a goat antibody against CAIX (R&D Systems) and a secondary anti-goat Alexa Fluor 488–coupled antibody (green fluorescence; Invitrogen). Nuclei were stained using 4′,6-diamidino-2-phenylindole (Sigma). Slices were examined with an Axioskop microscope (Zeiss) equipped for fluorescence, pictures were acquired using a charge-coupled device camera, and quantification of the signal intensity was done using ImageJ 1.37v.

Measurements of NO, Nitrite + Nitrate, and NOS Activity

Thoracic aorta were microdissected, placed in ice-cold physiologic solution [Krebs solution with 10 mmol/L Na-HEPES (pH 7.6)], and cleaned of all fat and connective tissue. The NO production was assayed by EPR spin trapping as described previously after formation of the paramagnetic adduct Fe(II)NO (diethyldithiocarbamate)$_2$ {[Fe(II)NO(DETC)$_2$]} in tissue treated for 30 min at 37°C with 0.4 mmol/L [Fe(II)(DETC)$_2$] complex as colloid and stimulated (or not) with ionomycin (2 μmol/L). For NO measurements by spin trapping, tissues were then rapidly frozen in calibrated tubes (0.3 mL) and kept in liquid nitrogen for EPR measurements. The EPR spectra were recorded with an X-band EMX at 77 K using a finger Dewar vial. A NO colorimetric assay (Roche Diagnostics) was used to determine the accumulation of NO derivatives (nitrite + nitrate) in the mouse plasma, muscle, or tumor. The activity of eNOS was also determined from embedded aorta rings by measuring the conversion of [³H]arginine to [³H]citrulline, as previously described (46). During the incubation period, embedded aortic rings were either maintained under normoxic conditions (21% O_2) or exposed to 95% O_2-5% CO_2 gas mixture in a modular incubator chamber.

Oxygenation Monitoring

EPR oximetry, using charcoal (CX0670-1, EM Science) or lithium phthalocyanine as oxygen-sensitive probes, was used to evaluate pO_2 levels in tumor and in collagen-embedded aorta, respectively, as previously described (42, 47).
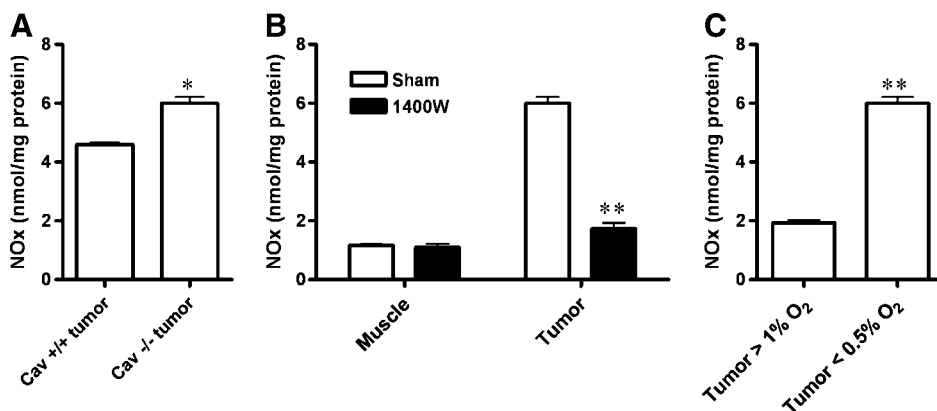

FIGURE 6. Nitrite production is promoted in hypoxic tumors. Bar graphs represent the extent of NO derivative [nitrite + nitrate (*NOx*)] production (**A**) in tumors grown in Cav$^{-/-}$ and Cav$^{+/+}$ mice (*, $P < 0.05$; $n = 3$), (**B**) in host tissue (muscle) or tumor isolated from sham- or 1400W-treated mice (**, $P < 0.01$; $n = 3$), and (**C**) in tumors with either >1% or <0.5% O_2 levels (**, $P < 0.01$; $n = 3$).

Statistical Analyses

Data are reported as mean ± SE, and statistical analyses were done using Student's *t* test or two-way ANOVA analyses where appropriate.

Disclosure of Potential Conflicts of Interest

No potential conflicts of interest were disclosed.

References

1. Moncada S, Higgs A, Furchgott R. International Union of Pharmacology Nomenclature in Nitric Oxide Research. Pharmacol Rev 1997;49:137–42.

2. Morbidelli L, Donnini S, Ziche M. Role of nitric oxide in the modulation of angiogenesis. Curr Pharm Des 2003;9:521–30.

3. Ignarro LJ, Fukuto JM, Griscavage JM, Rogers NE, Byrns RE. Oxidation of nitric oxide in aqueous solution to nitrite but not nitrate: comparison with enzymatically formed nitric oxide from L-arginine. Proc Natl Acad Sci U S A 1993;90: 8103–7.

4. Gladwin MT, Schechter AN, Kim-Shapiro DB, et al. The emerging biology of the nitrite anion. Nat Chem Biol 2005;1:308–14.

5. Crawford JH, Isbell TS, Huang Z, et al. Hypoxia, red blood cells, and nitrite regulate NO-dependent hypoxic vasodilation. Blood 2006;107:566–74.

6. Singel DJ, Stamler JS. Chemical physiology of blood flow regulation by red blood cells: the role of nitric oxide and *S*-nitrosohemoglobin. Annu Rev Physiol 2005;67:99–145.

7. Sonveaux P, Lobysheva II, Feron O, McMahon TJ. Transport and peripheral bioactivities of nitrogen oxides carried by red blood cell hemoglobin: role in oxygen delivery. Physiology (Bethesda) 2007;22:97–112.

8. Duranski MR, Greer JJ, Dejam A, et al. Cytoprotective effects of nitrite during *in vivo* ischemia-reperfusion of the heart and liver. J Clin Invest 2005;115: 1232–40.

9. Jung KH, Chu K, Ko SY, et al. Early intravenous infusion of sodium nitrite protects brain against *in vivo* ischemia-reperfusion injury. Stroke 2006;37: 2744–50.

10. Lu P, Liu F, Yao Z, et al. Nitrite-derived nitric oxide by xanthine oxidoreductase protects the liver against ischemia-reperfusion injury. Hepatobiliary Pancreat Dis Int 2005;4:350–5.

11. Tripatara P, Patel NS, Webb A, et al. Nitrite-derived nitric oxide protects the rat kidney against ischemia/reperfusion injury *in vivo*: role for xanthine oxidoreductase. J Am Soc Nephrol 2007;18:570–80.

12. Webb A, Bond R, McLean P, et al. Reduction of nitrite to nitric oxide during ischemia protects against myocardial ischemia-reperfusion damage. Proc Natl Acad Sci U S A 2004;101:13683–8.

13. Zweier JL, Wang P, Samouilov A, Kuppusamy P. Enzyme-independent formation of nitric oxide in biological tissues. Nat Med 1995;1:804–9.

14. Lundberg JO, Weitzberg E. NO generation from nitrite and its role in vascular control. Arterioscler Thromb Vasc Biol 2005;25:915–22.

15. Modin A, Bjorne H, Herulf M, et al. Nitrite-derived nitric oxide: a possible mediator of 'acidic-metabolic' vasodilation. Acta Physiol Scand 2001;171:9–16.

16. Zweier JL, Samouilov A, Kuppusamy P. Non-enzymatic nitric oxide synthesis in biological systems. Biochim Biophys Acta 1999;1411:250–62.

17. Cosby K, Partovi KS, Crawford JH, et al. Nitrite reduction to nitric oxide by deoxyhemoglobin vasodilates the human circulation. Nat Med 2003;9:1498–505.

18. Huang Z, Shiva S, Kim-Shapiro DB, et al. Enzymatic function of hemoglobin as a nitrite reductase that produces NO under allosteric control. J Clin Invest 2005;115:2099–107.

19. Godber BL, Doel JJ, Sapkota GP, et al. Reduction of nitrite to nitric oxide catalyzed by xanthine oxidoreductase. J Biol Chem 2000;275:7757–63.

20. Millar TM, Stevens CR, Benjamin N, et al. Xanthine oxidoreductase catalyses the reduction of nitrates and nitrite to nitric oxide under hypoxic conditions. FEBS Lett 1998;427:225–8.

21. Gautier C, van Faassen E, Mikula I, Martasek P, Slama-Schwok A. Endothelial nitric oxide synthase reduces nitrite anions to NO under anoxia. Biochem Biophys Res Commun 2006;341:816–21.

22. Vanin AF, Bevers LM, Slama-Schwok A, van Faassen EE. Nitric oxide synthase reduces nitrite to NO under anoxia. Cell Mol Life Sci 2007;64:96–103.

23. Feron O, Saldana F, Michel JB, Michel T. The endothelial nitric-oxide synthase-caveolin regulatory cycle. J Biol Chem 1998;273:3125–8.

24. Garcia-Cardena G, Fan R, Stern DF, Liu J, Sessa WC. Endothelial nitric oxide synthase is regulated by tyrosine phosphorylation and interacts with caveolin-1. J Biol Chem 1996;271:27237–40.

25. Ju H, Zou R, Venema VJ, Venema RC. Direct interaction of endothelial nitric-oxide synthase and caveolin-1 inhibits synthase activity. J Biol Chem 1997;272:18522–5.

26. Bucci M, Gratton JP, Rudic RD, et al. *In vivo* delivery of the caveolin-1 scaffolding domain inhibits nitric oxide synthesis and reduces inflammation. Nat Med 2000;6:1362–7.

27. Dewever J, Frerart F, Bouzin C, et al. Caveolin-1 is critical for the maturation of tumor blood vessels through the regulation of both endothelial tube formation and mural cell recruitment. Am J Pathol 2007;171:1619–28.

28. Regina A, Jodoin J, Khoueir P, et al. Down-regulation of caveolin-1 in glioma vasculature: modulation by radiotherapy. J Neurosci Res 2004;75:291–9.

29. Feron O, Belhassen L, Kobzik L, et al. Endothelial nitric oxide synthase targeting to caveolae. Specific interactions with caveolin isoforms in cardiac myocytes and endothelial cells. J Biol Chem 1996;271:22810–4.

30. Liu J, Razani B, Tang S, et al. Angiogenesis activators and inhibitors differentially regulate caveolin-1 expression and caveolae formation in vascular endothelial cells. Angiogenesis inhibitors block vascular endothelial growth factor-induced down-regulation of caveolin-1. J Biol Chem 1999;274:15781–5.

31. Li F, Sonveaux P, Rabbani ZN, et al. Regulation of HIF-1α stability through *S*-nitrosylation. Mol Cell 2007;26:63–74.

32. Biswas SK, Sica A, Lewis CE. Plasticity of macrophage function during tumor progression: regulation by distinct molecular mechanisms. J Immunol 2008; 180:2011–7.

33. Kashiwagi S, Tsukada K, Xu L, et al. Perivascular nitric oxide gradients normalize tumor vasculature. Nat Med 2008;14:255–7.

34. Fukumura D, Kashiwagi S, Jain RK. The role of nitric oxide in tumour progression. Nat Rev Cancer 2006;6:521–34.

35. Shiva S, Sack MN, Greer JJ, et al. Nitrite augments tolerance to ischemia/reperfusion injury via the modulation of mitochondrial electron transfer. J Exp Med 2007;204:2089–102.

36. Lundberg JO, Weitzberg E, Gladwin MT. The nitrate-nitrite-nitric oxide pathway in physiology and therapeutics. Nat Rev Drug Discov 2008;7:156–67.

37. Lin MI, Yu J, Murata T, Sessa WC. Caveolin-1-deficient mice have increased tumor microvascular permeability, angiogenesis, and growth. Cancer Res 2007; 67:2849–56.

38. Brouet A, Dewever J, Martinive P, et al. Antitumor effects of *in vivo* caveolin gene delivery are associated with the inhibition of the proangiogenic and vasodilatory effects of nitric oxide. FASEB J 2005;19:602–4.

39. Gratton JP, Lin MI, Yu J, et al. Selective inhibition of tumor microvascular permeability by cavtratin blocks tumor progression in mice. Cancer Cell 2003;4: 31–9.

40. Feron O, Dessy C, Opel DJ, et al. Modulation of the endothelial nitric-oxide synthase-caveolin interaction in cardiac myocytes. Implications for the autonomic regulation of heart rate. J Biol Chem 1998;273:30249–54.

41. Drab M, Verkade P, Elger M, et al. Loss of caveolae, vascular dysfunction, and pulmonary defects in caveolin-1 gene-disrupted mice. Science 2001;293: 2449–52.

42. Sonveaux P, Dessy C, Martinive P, et al. Endothelin-1 is a critical mediator of myogenic tone in tumor arterioles: implications for cancer treatment. Cancer Res 2004;64:3209–14.

43. Martinive P, Defresne F, Bouzin C, et al. Preconditioning of the tumor vasculature and tumor cells by intermittent hypoxia: implications for anticancer therapies. Cancer Res 2006;66:11736–44.

44. Masson VV, Devy L, Grignet-Debrus C, et al. Mouse aortic ring assay: a new approach of the molecular genetics of angiogenesis. Biol Proced Online 2002;4:24–31.

45. Sonveaux P, Martinive P, Dewever J, et al. Caveolin-1 expression is critical for vascular endothelial growth factor-induced ischemic hindlimb collateralization and nitric oxide-mediated angiogenesis. Circ Res 2004;95:154–61.

46. Piech A, Massart PE, Dessy C, et al. Decreased expression of myocardial eNOS and caveolin in dogs with hypertrophic cardiomyopathy. Am J Physiol Heart Circ Physiol 2002;282:H219–31.

47. Gallez B, Baudelet C, Jordan BF. Assessment of tumor oxygenation by electron paramagnetic resonance: principles and applications. NMR Biomed 2004;17: 240–62.